

# A New Laser Scan Method for Microstructural Control in Selective Laser Melting Process

Yong Son<sup>1</sup>, HyungGiun Kim<sup>2</sup>, Seung Ki Moon<sup>3</sup>, Il Hyuk Ahn<sup>\*4,5</sup>

<sup>1</sup>Digital Manufacturing Process Group, Korea Institute of Industrial Technology (KITECH), 113-58, Seohaean-ro, Siheung-si, Gyeonggi-do, 15014, South Korea

<sup>2</sup>Gangwon Regional Division, Korea Institute of Industrial Technology, Gangneung, 25440, South Korea

<sup>3</sup>School of Mechanical and Aerospace Engineering, Nanyang Technological University, 50 Nanyang Avenue, 639798, Singapore

<sup>\*4</sup>School of Mechanical Engineering, Tongmyong University, Busan, 48520, South Korea

<sup>5</sup>Center for Mechanical Convergence Engineering, Tongmyong University, Busan, 48520, South Korea

sonyong@kitech.re.kr<sup>1</sup>, hgk@kitech.re.kr<sup>2</sup>, skmoon@ntu.edu.sg<sup>3</sup>, ahnih@tu.ac.kr<sup>\*4,5</sup>

## Article Info

Volume 81

Page Number: 221 - 226

Publication Issue:

November-December 2019

## Abstract

**Background/Objectives:** In selective laser melting (SLM) process, laser scan pattern is one of most important parameters to understand the evolution of microstructures in a part. Mechanical properties of a fabricated part are highly dependent on the evolution of microstructure. Recently, some researchers have tried to control the microstructures by using diverse methods. This paper proposes a method based on overlap laser scanning technique to control the microstructure in a part.

**Methods/Statistical analysis:** This paper uses an overlap laser scanning technique. To implement the laser scan pattern, two different sets of laser power and scan speed are used. Default set has laser power (95W) and scan speed (125 mm/s), respectively. For overlap scan, 4 different sets are used. The representative Vickers hardness (Hv) for 5 different sets are determined by averaging 10 times measurement. The representative values are compared for the effectiveness of proposed overlap scan method. To understand the change of Vickers hardness with the different sets, the size and shape of acicular  $\alpha'$  martensite and the concentration of O and N elements are observed.

**Findings:** From the measurements, Vickers hardness increases with the energy density for the overlap laser scan by about 18%, comparing to one without overlap laser scan. With the increase of the energy density for overlap laser scan, the refinement of the acicular  $\alpha'$  martensite increases. The change of the hardness shows the similar tendency with the change of the concentration of O and N elements.

**Improvements/Applications:** The results of this paper show the possibility of the microstructure design. It can also improve the design freedom by freely assigning the mechanical properties.

**Keywords:** Additive manufacturing, Selective laser melting, Microstructure design, Overlap laser scanning

## Article History

Article Received: 3 January 2019

Revised: 25 March 2019

Accepted: 28 July 2019

Publication: 22 November 2019

## I. Introduction

As one of promising metal additive manufacturing (AM) technologies, selective laser melting (SLM) process is widely adopted, due to the dimensional accuracy and the mechanical properties [1-3]. In the SLM process, Ti-6Al-4V is one of important metallic materials, thanks to the high specific strength and the biocompatibility [4-7]. The mechanical properties of selective laser melted Ti-6Al-4V part significantly depend on evolving microstructure such as the constituent phase, the morphology, the size and orientation of the prior  $\beta$ -grains, and the characteristic lengths of  $\alpha'$  martensite grown within the prior  $\beta$ -grains [8-10]. The evolution of the microstructure is very sensitive to heat transfer histories [11-13]. Among many process parameters in SLM process, there are three important process parameters such as laser power (W), scan speed (mm/s) and hatch spacing (mm) to influence thermal-physical phenomenon [14, 15]. Depending on the three process parameters, a melt pool, a liquid phase of metallic powders, has different heat distributions and cooling rate, leading to forming the different microstructure. It means that microstructures can be controlled by adjusting the process parameters. The ability of controlling the microstructures in the SLM process could improve the performance of components or functional parts [16, 17]. Many researchers have studied the evolution of the microstructure with various parameters [18-21]. From the recent literature, it can be found that diverse parameters have been used to change the microstructures to assign functionalities to volumes or surfaces of a part. Until now, however, a few of researches have performed the works, because the specific scan strategies in the commercialized SLM machine cannot be implemented. Thus, in developing the scan strategy to control the microstructure in a part, the applicability of a new scan strategy to the SLM machine should be considered.

In this regard, this paper proposes a method to selectively change microstructures within a

part, based on the commercialized SLM machine. Specimens are fabricated with the proposed method and the fabricated specimens are analyzed to verify the usefulness of the proposed method by identifying the change of hardness, microstructures and the chemical composition.

## II. Materials and Methods

In this paper, specimens were fabricated by SLM 250HL system with a spot size of 80  $\mu\text{m}$  diameter. Working chamber is filled with argon gas and sustained with the oxygen content ( $<0.2\%$ ). Substrate on working platform is heated up to 200  $^{\circ}\text{C}$  to alleviate the thermal gradient. Ti-6Al-4V powders with the particle size from 20  $\mu\text{m}$  to 63  $\mu\text{m}$  were used. Two different sets of process parameters were used for the specimen fabrications. A default set of process parameters, including laser power (W) and scan speed (mm/s), is determined based on the values obtained from optimization experiments carried out in Singapore center for 3D Printing (SC3DP).

In addition, four additional sets of process parameters are used to selectively control microstructure. For the four additional sets, the optimization for hatch spacing (mm) was performed based on the relative density. The results measured for the relative densities are summarized in Table 1. Figure 1 shows the procedure of specimen fabrication. The fabricated specimens were polished and then were etched with Kroll's reagent (10 mL of HF, 30 mL of  $\text{HNO}_3$  and 50 mL of water) for 4~5 seconds. To investigate the change of mechanical property with microstructures, Vickers micro-hardness tests were conducted by using a Future Tech FM-300e micro hardness testers on a load of 500g and 15sec dwell time. To obtain the microstructural characterization, scanning electron microscopy (SEM, JEOL JMS 6700F) were utilized. To identify the reason for the change of mechanical property from the chemical composition variation, the amount of oxygen and nitrogen in a specimen were measured by O/N analyzer (LECO, 763 series).

**Table 1 : Relative densities with different sets of process parameters**

Set	Energy density (W/mm.s <sup>-1</sup> )	P (W)	V (mm/s)	Hatch spacing (mm)						Note	
				0.10	0.11	0.12	0.13	0.14	0.15		0.16
C <sub>0</sub>	E <sub>0</sub>	95	125	0.987	0.989	0.988	0.984	0.984	0.987	0.984	Default part
C <sub>1</sub>	2·E <sub>0</sub>	195	125	0.988	0.981	0.991	0.988	0.976	0.977	0.984	
C <sub>2</sub>	2·E <sub>0</sub>	95	63	0.990	0.991	0.989	0.988	0.989	0.967	0.985	Overlap part
C <sub>3</sub>	1/2·E <sub>0</sub>	95	250	0.980	0.983	0.973	0.972	0.981	0.977	0.968	part
C <sub>4</sub>	1/2·E <sub>0</sub>	48	125	0.919	0.936	0.896	0.930	0.903	0.892	0.921	

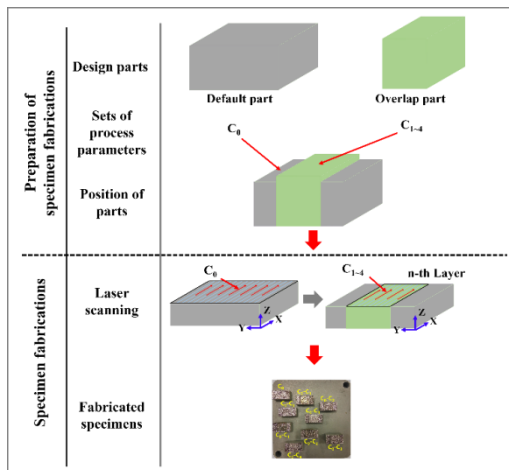


**Figure1. Schematic diagram for specimen fabrication in the proposed method**

**III. Results and Discussion**

Vickers hardness is measured to investigate the change of mechanical property in overlap area with energy densities from C<sub>1</sub> to C<sub>4</sub> cases. In each case, hardness measurements along the

middle of specimens are conducted. The representative value in a position is calculated by averaging 10 measurements. For all cases, measured results are shown in Figure 2.

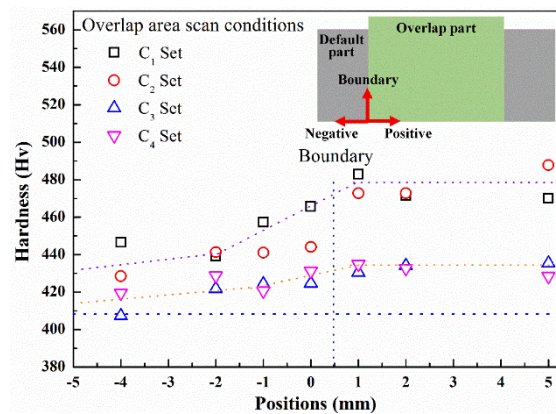


**Figure 2. Variation of Vickers hardness with positions**

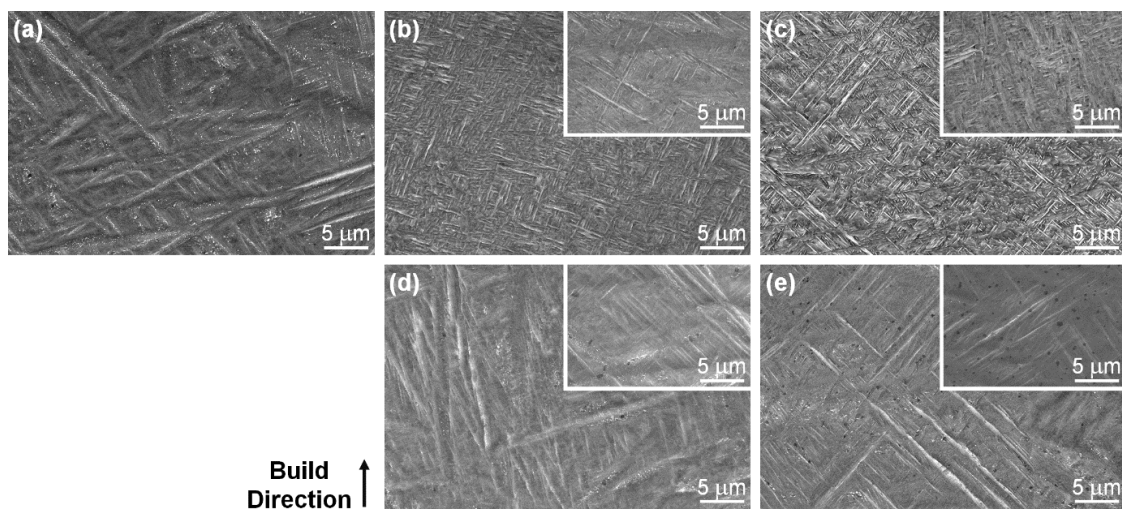


**Figure3. SEM images of (a) C<sub>0</sub>, (b) C<sub>1</sub>, (c) C<sub>2</sub>, (d) C<sub>3</sub>, and (e) C<sub>4</sub>. Non-overlap area of C<sub>1</sub>~C<sub>4</sub> sets were inset, respectively.**

From Figure 2, two phenomena can be observed. First, it can be seen that the laser scanning for overlap area (hereafter, called “overlap laser scanning”) causes the increase of hardness. In the center of specimens, hardness is increased by about 70~80 Hv in C<sub>1</sub> and C<sub>2</sub> cases, and by about 20~30 Hv in C<sub>3</sub> and C<sub>4</sub> cases, comparing to hardness in C<sub>0</sub> set (401 Hv). The change of the hardness can be explained by investigating the refinement of the acicular  $\alpha'$  martensite caused by the heat transferred from the overlap laser scanning [18, 22]. Figure 3 shows the refining effect increases with the increase of the energy density for the overlap laser scanning, and proves that the refinement of the acicular  $\alpha'$  martensite can affect the change of the hardness. However, there are no significant differences in cases with the same energy densities (C<sub>1</sub> and C<sub>2</sub>, or C<sub>3</sub> and C<sub>4</sub>). It means that the increase of the hardness is only dependent on the energy density. In addition, the refinement effect by only thermal heat treatment was reported in the previous studies on the mechanical property and microstructure of conventional Ti-6Al-4V alloy (23-25). Second, hardness is gradually decreased along positions from positive to negative in all cases with overlapped area. The degree of the decrease of the hardness is dependent on the energy density for the overlap laser scanning. In C<sub>1</sub> and C<sub>2</sub> cases, hardness in non-overlap area is still higher than one in C<sub>0</sub> case. However, in C<sub>3</sub> and C<sub>4</sub> cases, hardness in the edge of the default area is comparable with hardness measured in C<sub>0</sub> case. It means that the reheating caused by the overlap scanning affects the formation of the microstructures outside of the overlap area, and the range of the reheating effect depends on the energy density for the overlap laser scanning. The insets of Figure 3 prove that the reheating effect leads to refine the acicular  $\alpha'$  martensite in cases with overlap area, and the degree of the reheating effect is changed with the energy density of the overlap scanning. Microstructural control including the grain size, phase, and aspect ratio is possible using the variable heating and cooling conditions

with temperature, time and number of heat treatment times, then it could be affected to the mechanical properties [26, 27].

Additionally, in viewpoint of the chemical composition, oxygen and nitrogen were measured to explain the change of hardness with the energy density. The results are plotted in Figure 4. Hardness in Figure 4 is used in measured in the center of the overlap area. From Figure 4, it can be obtained that the change of the hardness is similar to the change of the amount of oxygen and nitrogen. It shows that the solid-solution hardening is the main hardening mechanism for the increase of the hardness and the degree of the solid-solution hardening is also dependent on the energy density [28].

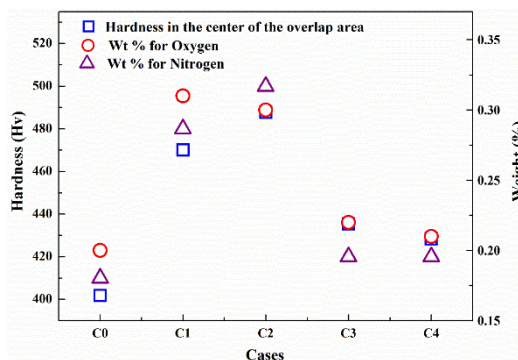


**Figure 4. Comparison between hardness in the center of the overlap area and the amount of oxygen/nitrogen with the energy density of the overlap laser scanning**

From the results above, it can be concluded that the overlap laser scanning can change microstructures and the amount of oxygen and nitrogen, resulting in changing hardness. It means that mechanical properties can be selectively controlled by the proposed method. The conclusions can be utilized to improve the performance of the component fabricated by SLM process. When a component is designed, engineer has used a material with homogeneous mechanical properties. However, if mechanical properties can be selectively controlled by using the proposed laser scanning method, engineer should consider a surface or a volume as a functional unit in component design, and can design a high performance component with a material [29,

30]. Furthermore, the in-situ heat treatments by means of the overlap laser scanning could simply applied on the SLM process for the practical use, thus the study on additional effects of diverse conditions would be remained for the future works.

#### IV. Conclusion

This paper proposed a new laser scanning method, based on overlapping parts with different laser energy densities. In specimens fabricated with the proposed method, hardness of specimens with overlap area is higher than one of specimens without overlap area. The increase of hardness is dependent on the energy density for overlap laser scanning, and the increase is caused by the refinement of the acicular  $\alpha'$  martensite and the increase of the concentration of light elements such as oxygen and nitrogen.

In future work, authors will study the relationship between energy density for overlap area and the evolution of microstructure to delicately control microstructures in which engineer want to assign different mechanical property.

#### V. Acknowledgment

The research was partially supported by Industrial Technology Innovation Program funded by MOTIE and KEIT (Project Number: 20000201), KITECH (Korea Institute of Industrial Technology) internal project, Singapore Centre for 3D Printing (SC3DP), and National Research Foundation, Singapore and the National Research Foundation of Korea (Grant NRF-2018R1D1A1B07048284)

#### References

- [1] Spierings AB, Herres N, Levy G. Influence of the particle size distribution on surface quality and mechanical properties in AM steel parts. *Rapid Prototyping J.* 2011;17(3):195-202.
- [2] Sun J, Yang Y, Wang D. Mechanical Properties of Ti-6Al-4V Octahedral Porous Material Unit Formed by Selective Laser Melting. *ADV MECH ENG.* 2015;4(0):427386-.
- [3] Sun J, Yang Y, Wang D. Mechanical properties of a Ti6Al4V porous structure produced by selective laser melting. *Mater Des.* 2013;49:545-52.
- [4] Biemond JE, Hannink G, Verdonschot N, Buma P. Bone ingrowth potential of electron beam and selective laser melting produced trabecular-like implant surfaces with and without a biomimetic coating. *Journal of materials science Materials in medicine.* 2013;24(3):745-53.
- [5] Zhang LC, Klemm D, Eckert J, Hao YL, Sercombe TB. Manufacture by selective laser melting and mechanical behavior of a biomedical Ti-24Nb-4Zr-8Sn alloy. *Scr Mater.* 2011;65(1):21-4.
- [6] Xiao D, Yang Y, Su X, Wang D, Sun J. An integrated approach of topology optimized design and selective laser melting process for titanium implants materials. *Biomed Mater Eng.* 2013;23(5):433-45.
- [7] Van der Stok J, Van der Jagt OP, Amin Yavari S, De Haas MF, Waarsing JH, Jahr H, et al. Selective laser melting-produced porous titanium scaffolds regenerate bone in critical size cortical bone defects. *Journal of orthopaedic research : official publication of the Orthopaedic Research Society.* 2013;31(5):792-9.
- [8] Chlebus E, Kuźnicka B, Kurzynowski T, Dybała B. Microstructure and mechanical behaviour of Ti-6Al-7Nb alloy produced by selective laser melting. *Mater Charact.* 2011;62(5):488-95.
- [9] Sallica-Leva E, Jardini AL, Fogagnolo JB. Microstructure and mechanical behavior of porous Ti-6Al-4V parts obtained by selective laser melting. *Journal of the mechanical behavior of biomedical materials.* 2013;26:98-108.
- [10] Thijs L, Verhaeghe F, Craeghs T, Humbeeck JV, Kruth J-P. A study of the microstructural evolution during selective laser melting of Ti-6Al-4V. *Acta Mater.* 2010;58(9):3303-12.
- [11] Vrancken B, Thijs L, Kruth J-P, Van Humbeeck J. Heat treatment of Ti6Al4V produced by Selective Laser Melting:

- Microstructure and mechanical properties. *J Alloys Compd.* 2012;541:177-85.
- [12] Vilaro T, Colin C, Bartout JD, Nazé L, Sennour M. Microstructural and mechanical approaches of the selective laser melting process applied to a nickel-base superalloy. *Mater Sci Eng, A.* 2012;534:446-51.
- [13] Thijs L, Montero Sistiaga ML, Wauthle R, Xie Q, Kruth J-P, Van Humbeeck J. Strong morphological and crystallographic texture and resulting yield strength anisotropy in selective laser melted tantalum. *Acta Mater.* 2013;61(12):4657-68.
- [14] Clijsters S, Craeghs T, Buls S, Kempen K, Kruth J-P. In situ quality control of the selective laser melting process using a high-speed, real-time melt pool monitoring system. *INT J ADV MANUF TECH.* 2014;75(5-8):1089-101.
- [15] Ahn IH, Moon SK, Hwang J, Bi G. Characteristic length of the solidified melt pool in selective laser melting process. *Rapid Prototyping J.* 2017;23(2):370-81.
- [16] Gibson I, Rosen DW, Stucker B. *Additive manufacturing technologies*: Springer; 2010.
- [17] Bourell D, Kruth JP, Leu M, Levy G, Rosen D, Beese AM, et al. *Materials for additive manufacturing*. CIRP ANN-MANUF TECHN. 2017.
- [18] Yang J, Yu H, Yin J, Gao M, Wang Z, Zeng X. Formation and control of martensite in Ti-6Al-4V alloy produced by selective laser melting. *Mater Des.* 2016;108:308-18.
- [19] Simonelli M, Tse YY, Tuck C. The formation of  $\alpha + \beta$  microstructure in as-fabricated selective laser melting of Ti-6Al-4V. *J Mater Res.* 2014;29(17):2028-35.
- [20] Xu W, Sun S, Elambasseril J, Liu Q, Brandt M, Qian M. Ti-6Al-4V additively manufactured by selective laser melting with superior mechanical properties. *JOM.* 2015;67(3):668-73.
- [21] Körner C, Helmer H, Bauereiß A, Singer RF, editors. Tailoring the grain structure of IN718 during selective electron beam melting. *MATEC Web Conf*; 2014: EDP Sciences.
- [22] Park HK, Ahn YK, Lee BS, Jung KH, Lee CW, Kim HG. Refining effect of electron beam melting on additive manufacturing of pure titanium products. *Mater Lett.* 2017;187:98-100.
- [23] Morita T, Hatsuoka K, Iizuka T, Kawasaki K. Strengthening of Ti-6Al-4V alloy by short-time duplex heat treatment. *Mater Trans.* 2005;46(7):1681-6.
- [24] ZHANG A-l, Dong L, Tang H-b, Wang H-m. Microstructure evolution of laser deposited Ti60A titanium alloy during cyclic thermal exposure. *Trans Nonferrous Met Soc China.* 2013;23(11):3249-56.
- [25] Tanaka S, Morita T, Shinoda K, editors. *Effects of Short-Time Duplex Heat Treatment on Microstructure and Fatigue Strength of Ti-6Al-4V Alloy*. ICF13; 2013.
- [26] Szkliniarz W, Chrapoński J, Kościelna A, Serek B. Substructure of titanium alloys after cyclic heat treatment. *Mater Chem Phys.* 2003;81(2):538-41.
- [27] Shackelford JF, Muralidhara MK. *Introduction to materials science for engineers*: Pearson Education; 2015.
- [28] Vilaro T, Colin C, Bartout J-D. As-fabricated and heat-treated microstructures of the Ti-6Al-4V alloy processed by selective laser melting. *Metall Mater Trans A.* 2011;42(10):3190-9.
- [29] Yang S, Tang Y, Zhao YF. A new part consolidation method to embrace the design freedom of additive manufacturing. *J Manuf Process.* 2015;20:444-9.
- [30] Yang S, Zhao Y. Additive manufacturing-enabled design theory and methodology: a critical review. *INT J ADV MANUF TECH.* 2015;80.